



Universität Potsdam

C. Dosche, M. U. Kumke, H.-G. Löhmansröben, F. Ariese,
A. N. Bader, C. Gooijer, O. S. Miljanic, M. Iwamoto,
K. P. C. Vollhardt, R. Puchta and N. J. R. van Eikema Hommes

Deuteration effects on the vibronic structure of the fluorescence spectra and the internal conversion rates of triangular [4]Phenylene

first published in:

Physical chemistry, chemical physics : PCCP ; a journal of European chemical societies. -
ISSN 1463-9076. - 6 (2004), S. 5476 - 5483

doi: 10.1039/b414545c

Postprint published at the institutional repository of Potsdam University:

In: Postprints der Universität Potsdam : Mathematisch-Naturwissenschaftliche
Reihe 1 (2006), 002

<http://opus.kobv.de/ubp/volltexte/2006/1188/>

<http://nbn-resolving.de/urn:nbn:de:kobv:517-opus-11881>

Postprints der Universität Potsdam
Mathematisch-Naturwissenschaftliche Reihe
1 (2006) 002

Deuteration effects on the vibronic structure of the fluorescence spectra and the internal conversion rates of triangular [4]Phenylene

C. Dosche,^a M. U. Kumke,^a H.-G. Löhmansröben,^{a*} F. Ariese,^b A. N. Bader,^b C. Gooijer,^b O. Š. Miljanić,^c M. Iwamoto,^c K. P. C. Vollhardt,^c R. Puchta^d and N. J. R. van Eikema Hommes^d

^a *Institute of Chemistry, University of Potsdam, Karl-Liebknecht-Str. 24-25, 14476 Golm, Germany*

^b *Department of Analytical Chemistry and Applied Spectroscopy, Vrije Universiteit, De Boelelaan 1083, 1081 HV Amsterdam, The Netherlands*

^c *Center for New Directions in Organic Synthesis, Department of Chemistry, University of California at Berkeley and the Chemical Sciences Division, Lawrence Berkeley National Laboratory, Berkeley, California, 94720-1460, USA*

^d *Computer-Chemie-Centrum, Universität Erlangen-Nürnberg, Nögelsbachstr. 25, 91052 Erlangen, Germany*

Deuteration effects on the vibronic structure of the emission and excitation spectra of triangular [4]phenylene (D_{3h} [4]phenylene) were studied using laser-excited Shpol'skii spectroscopy (LESS) in an octane matrix at 4.2 K. For correct assignment of the vibrational modes, the experimental results were compared with calculated frequencies (B3LYP/6-31G*). CH vibrations were identified by their characteristic isotopic shift in the spectra of deuterated triangular [4]phenylenes. Two CC stretching modes, at 100 cm^{-1} and 1176 cm^{-1} , suitable as probes for bond strength changes in the excited state, were identified. The isotope effect on the internal conversion rates of triangular [4]phenylene was evaluated from temperature dependent lifetime measurements. Isotope dependency and the magnitude of the internal conversion rates indicate that internal conversion in triangular [4]phenylene is most likely induced by CH vibrations. The results obtained by LESS and lifetime measurements were compared with PM3 PECI calculations of the excited state structure. The theoretical results and the relation between ground and excited state vibration energies of the 1176 cm^{-1} probe

vibration indicate a reduction of bond alternation of the central cyclohexatriene ring in the excited state.

1. Introduction

The nature of aromaticity in benzene has been subject of theoretical and experimental investigations for decades and is still of high priority for research, as evident from recent review issues.* A new aspect was added to this discussion with the assignment of the so called Kekule mode in the vibronic structure of the electronic S_0 - and S_1 -state of benzene.¹ One explanation for the abnormal shift of this vibration to higher energies in the S_1 -state was the concept of the excited twin state introduced by Shaik.²⁻⁵ This model suggested that the delocalization of the CC-bonds in benzene is enforced by the σ -system, whereas the π -system tends to adopt a localized structure. Recently it was pointed out that benzene systems that are deformed in a cyclohexatriene-type manner by clamping groups, would undergo a restoration of the benzene structure in the S_1 -state.²⁻⁵

Similarly deformed are the central rings of angular [N]phenylenes, such as the triangular [4]phenylene (**1**). [N]phenylenes consist of alternating condensed benzenoid and cyclobutadienoid rings, which can be connected in a linear or angular manner. However, it has been theoretically shown that, in contrast to deformed benzene systems with saturated clamping groups like the well known Siegel compound (**2**), the central ring of angular [N]phenylenes does not exhibit any aromatic ring current.⁶ Due to their special structural and electronic properties, [N]phenylenes have been subjects of several theoretical studies concerning the aromaticity of condensed hydrocarbons.⁶⁻¹⁵ A central aspect of the theoretical investigations is the interplay between their respective aromatic and antiaromatic character. Because of the anti-aromatic character of the cyclobutadienoid rings, the electron density in the π -bonds shared by six-membered and four-membered rings is reduced, resulting in a weakening and elongation of these bonds. If the π -bond length is enlarged in an alternating manner, as in the angular [N]phenylenes, the central six-membered ring will be deformed in a cyclohexatriene-type way, with the effect being maximal for (**1**). As a result of the influence of the cyclobutadienoid rings, the aromatic character of the central ring changes to a non aromatic system, which can be measured in terms of NMR-shifts or vibrational energies.

*Chem. Rev. **101** (2001), 5
Phys. Chem. Chem. Phys. **6** (2004), 2

Indeed, the calculated NICS values and π -ring current maps for (**1**) suggest that the central ring is not aromatic by these criteria.^{6,8,13,15}

After the synthesis of [N]phenylenes of various topologies,¹⁶⁻²⁸ the experimental confirmation of the theoretical data has become possible. The cyclohexatriene nature of the central ring of (**1**) in the ground state has been demonstrated experimentally by the chemical reactivity of this compound^{29,30} and the X-ray diffraction data.¹⁹ Information about the electronically excited states can be obtained by stationary and time resolved fluorescence spectroscopy. First photophysical studies revealed some unusual spectroscopic properties of the [N]phenylenes.³¹ The most interesting result is the striking difference in the rate constants of radiationless deactivation via internal conversion (k_{IC}), which are in the range of 10^7 s⁻¹ for angularly annelated [N]phenylenes and 10^{10} s⁻¹ for linearly annelated [N]phenylenes. It was suggested that this difference is mainly connected to the Franck-Condon factors between vibronic modes of the S₁- and the S₀-state.³¹ Therefore, an analysis of the vibronic structure of the fluorescence and absorption spectra of [N]phenylenes is necessary. Concerning the influence of the annelation geometry on the Franck-Condon factors, it was suspected that for angular [N]phenylenes the coupling between S₀- and S₁-state is induced mainly by CH valence vibrations, as is the case for “classical” polycyclic aromatic hydrocarbons, whereas for linear [N]phenylenes, as well as for the parent compound biphenylene, the radiationless deactivation processes seem to be a result of CC stretching modes.³¹⁻³⁵ To verify this assumption, the influence of deuteration on k_{IC} and the vibronic structure of electronic spectra of angular [N]phenylenes was studied for triangular [4]phenylene (**1**)-*h*₁₂, (**1**)-*d*₆ and (**1**)-*d*₁₂ (Fig. 1).

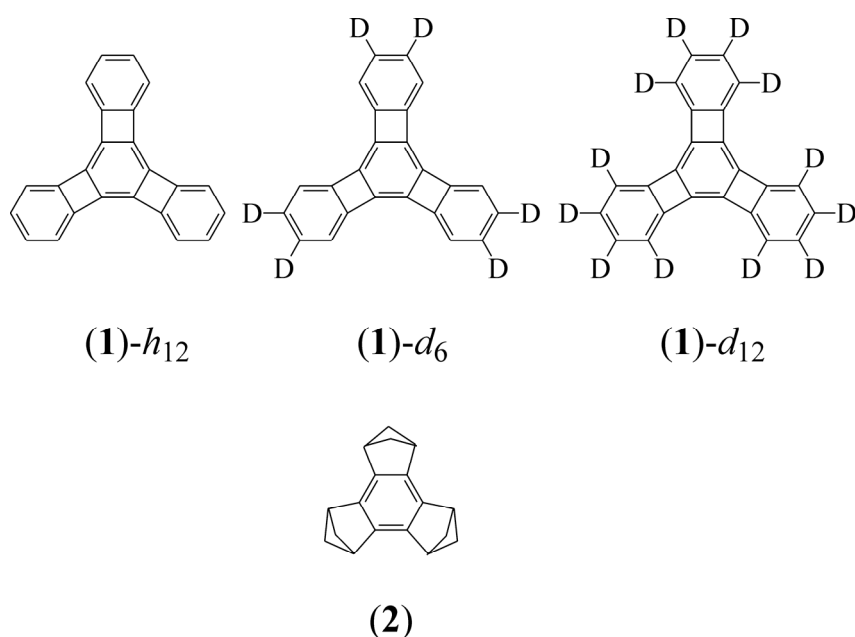


Fig. 1: Structures of the triangular [4]phenylenes (**1**) and the Siegel compound (**2**)

Recently, the suitability of laser-induced Shpol'skii spectroscopy (LESS) for the analysis of the vibronic structure of [N]phenylene fluorescence emission and excitation spectra was demonstrated.³⁶ Although information about ground state vibrations can be obtained by Raman or IR spectroscopy as well, LESS can provide important additional data. Apart from different selection rules, the advantage of LESS is the experimental access to excited state vibrations via the fluorescence excitation spectra. Using this method, a direct comparison of ground and excited state is possible. In addition to the experimental results, DFT calculations were performed. As experimental and theoretical data were in good agreement, the assignment of the observed vibrational modes to the calculated nuclear movement patterns was possible. These results led to the identification of a low-frequency, in-plane vibration located around 100 cm^{-1} , which is a unique feature of angular [N]phenylenes. As this vibration causes a deviation in the bending angle formed by the centers of three benzenoid rings in an angular annelated [N]phenylene, it may be involved in the rapid enantiomerisation of helical [N]phenylenes.^{12,27,28,36} Apart from these results, the facile in-plane deformation of [N]phenylenes has been demonstrated separately on biphenylene with strained substituents.³⁷ Although the nature of the corresponding deformation vibration is still not clear, the theoretical results indicate that it is connected to the cyclobutadienoid rings. From this point of view, the low-frequency vibration - like other vibrations caused by these rings - is of great interest as a diagnostic tool for the characterization of their properties. Apart from the low frequency deformation vibration, the most interesting vibrational modes are CC valence vibrations in the cyclobutadienoid parts of [N]phenylene molecules. IR-data of biphenylene indicate that these modes are located in the range between 1200 and 1300 cm^{-1} .^{38,39} Comparison of the vibrational frequencies of biphenylene and angular [N]phenylenes could shed light on the influence of the cyclohexatriene-type stabilisation on the cyclobutadienoid rings observed in angular [N]phenylenes.^{7-13,19-28,40} However, the exact assignment of these vibronic bands in [N]phenylene Shpol'skii spectra in the region of 1100 - 1300 cm^{-1} is difficult due to overlap with in-plane CH bending modes located in this region. In addition, vibrational analysis of the emission spectra is complicated by overlapping multiplets. This multiplet structure is due to different possible orientations of the guest molecules in the Shpol'skii matrix.^{41,42} LESS is therefore necessary for the selective excitation of molecules in distinct sites.

In this study, we present site-selective Shpol'skii excitation and emission spectra of (**1**)-*h*₁₂ and its semi- and completely deuterated isotopomers (**1**)-*d*₆ and (**1**)-*d*₁₂, the former being selectively deuterated at the β positions. From additional DFT calculations, CC stretching

modes of the cyclobutadienoid rings in the ground and excited state are identified and compared with the corresponding values for biphenylene. Apart from the effect of deuteration on the vibronic structure of the fluorescence spectra, the influence of deuteration on internal conversion rates of (1)- h_{12} and (1)- d_{12} is evaluated via the temperature dependence of fluorescence lifetimes.

2. Experimental section

Phenylene (1) was prepared and characterized according to the literature.²⁰ For the synthesis of (1)- d_{12} , the method from Ref. 20 was modified regarding the desilylation steps in the synthesis of (1)- h_{12} . (1)- d_6 was prepared by desilylation of the hexakis(trimethylsilyl) precursor of (1) with CF_3COOD . For detailed synthesis procedures see below. [N]Phenylene concentrations were $\sim 5 \times 10^{-6}$ mol/L for Shpol'skii measurements and 10^{-5} mol/L for fluorescence lifetime measurements. [N]Phenylenes were dissolved in HPLC grade 2-methyltetrahydrofuran (Aldrich, Taufkirchen, Germany) for lifetime measurements and in HPLC grade octane (Fluka, Buchs, Switzerland) for Shpol'skii measurements.

IR-spectra were obtained in a CsI matrix using a NEXUS-FT-IR spectrometer (Thermo Nicolet, Madison, USA).

For lifetime measurements at different temperatures, the samples were prepared in a 5x5mm home-built monolithic quartz cell, deoxygenated by flushing the samples 15 min with argon, and then cooled to 80 - 280 K with an Optistate DN1704 cryostat (Oxford Instruments, Wiesbaden, Germany) fitted with an external controller (ITC4; Oxford Instruments). Lifetime measurements were performed with an FL920 fluorimeter (Edinburgh Instruments, Livingston, UK). A frequency doubled titanium sapphire laser system (Tsunami 3960; Spectra Physics, Mountain View, USA) set at 392 nm was used as the excitation light source. The original repetition rate of 80 MHz was reduced to 500 kHz with a pulse picker (Pulse Select; APE, Berlin, Germany). Fluorescence was detected with a multichannel plate (ELDY EM1-132/300, Europhoton, Berlin, Germany), providing a time response of ~ 100 ps.

For Shpol'skii measurements, the sample solutions were filled in 4x50 mm quartz tubes, sealed with rubber septa and then cooled to 4 K in a lab built sample holder that was mounted to a closed cycle helium refrigerator (SRDK-205 cryostat; Janis Research Company, Wilmington, MA, USA). The samples were excited using a dye laser (LPD 3002; Lambda Physik, Göttingen, Germany) pumped by a XeCl-excimer laser (LPX 110i; Lambda Physik). The excitation wavelength was varied between 410 and 445 nm using POPOP as laser dye. The laser was operated at 20 Hz with a pulse width of 10 ns. The fluorescence emission was

collected at a 90° angle to the excitation light by a 3 cm F/1.2 quartz lens and focused on the entrance slit of a triple monochromator (Spex 1877; Edison, NJ, USA) by a 10 cm F/4 quartz lens. For detection, an intensified CCD-camera (DH720-25U-03; Andor Technologies, Belfast, UK) was used in gated mode. The achieved spectral resolution was 0.1 nm in a 36 nm window. For wavelength calibration, an argon arc lamp was used. In order to obtain adequate stray light suppression, delay and gate width were set to 50 ns and 2 μ s, respectively.

The excitation spectra were reconstructed from cross sections at 451 nm of a time series of emission spectra. Each emission spectrum was accumulated over 20 pulses within a 1 s time period. The excitation wavelength was varied with a scan rate of 0.05 nm/s. For site-selective emission spectra, the samples were excited at the wavelength of the main site of the second vibronic band located around 434 nm in the excitation spectra and accumulated over 100 pulses.

All spectra were corrected for the background signal of the iCCD-camera collected over 20 and 100 pulses, respectively.

The fundamental vibrations of the [N]phenylenes were calculated using density functional theory. Calculations were carried out with Gaussian 98 using the B3LYP method and the 6-31G* basis set.⁴³⁻⁴⁷ The results were corrected with a factor of 0.96 for out-of-plane modes and 0.97 for in-plane modes.⁴⁸ Excited state geometries were determined using PM3 PECl calculations performed with VAMP 8.1.⁴⁹⁻⁵²

3. Results and Discussion

Shpol'skii spectra of (1)-*h*₁₂, (1)-*d*₆ and (1)-*d*₁₂ were recorded under site selective conditions. For vibrational analysis, the spectra were normalized to the 0-0 transition in the energy scale. The average error of the peak positions is about ± 5 cm⁻¹.

3.1 Vibrational analysis of Shpol'skii emission spectra

The recorded emission spectra are depicted in Fig. 2. For assignment of the distinct vibronic bands and for separation of CC and CH vibrations, the experimental values are compared with the DFT calculations. The experimental and theoretical results are summarized in Tab. 1.

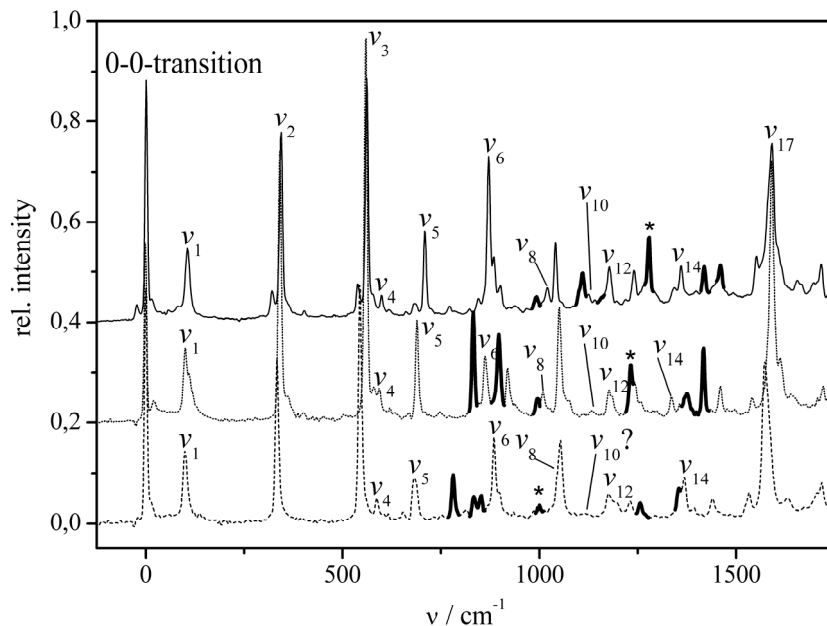


Fig. 2: Shpol'skii emission spectra ($\lambda_{\text{ex}} = 434 \text{ nm}$) of **(1)- h_{12}** (solid), **(1)- d_6** (dotted) and **(1)- d_{12}** (dashed) at 4.2 K in octane. Vibrational energies (given in cm^{-1}) of the vibronic bands are given relative to the 0-0-transition. CC vibrations are labeled, CH vibrations are marked as bold lines. For demonstration of the isotopic effect, ν_{13} is separately marked (*).

mode	$\nu(S_0) / \text{cm}^{-1}$	$\nu(S_1) / \text{cm}^{-1}$	DFT
ν_1	105 (o.r.)	92	103
	99 (o.r.)	91	99
	99 (o.r.)	89	97
ν_2	344 (350)	333	337
	340 (349)	329	332
	333 (335)	323	325
ν_3	560 (561)	557	554
	559 (555)	547	549
	543 (539)	534	535
ν_4	598 (598)	580	593
	592 (n.o.)	569	586
	586 (n.o.)	575	579
ν_5	708 (704)	682	704
	689 (684)	662	680
	681 (681)	657	672
ν_6	871 (875)	853	872
	862 (850)	839	883
	882 (881)	863	876
ν_7	991 (997)	974	995
	997 (991)	981	991
	780 (764)	766	776
ν_8	1019 (1036)	993	1026
	1011 (1039)	1002	1033
	1045 (1044)	1033	1039

ν_9	1110 (1110) 897 (n.o.) 852 (850)	1088 872 840	1106 906 840
ν_{10}	1125 (1130) 1134 (1126) 1118 (1114)	1113 1116 1080	1130 1129 1112
ν_{11}	1161 (1153) 832 (829) 833 (833)	1151 822 830	1156 821 824
ν_{12}	1176 (1168) 1177 (1166) 1175 (1165)	1178 1182 1174	1179 1170 1162
ν_{13}	1279 (1278) 1233 (1232) 995 (991)	1266 1220 990	1275 1229 978
ν_{14}	1359 (1359) 1334 (1328) 1368 (1354)	1319 1324 1329	1372 1344 1371
ν_{15}	1419 (1419) 1417 (1411) 1258 (1290)	1348 1372 1272	1424 1418 1296
ν_{16}	1460 (1456) 1375 (1365) 1355 (1349)	1436 1356 1324	1459 1369 1350
ν_{17}	1591 (n.o.) 1590 (1568) 1573 (1559)	1531 1524 1505	1587 1577 1563

Tab. 1: S_0 -state, S_1 -state and calculated vibrational energies of e' -modes of (1)- h_{12} (upper), (1)- d_6 (middle) and (1)- d_{12} (lower) given in cm^{-1} . Vibrational energies taken from IR-spectra are given in brackets (o.r.: out of range; n.o.: not observed). CH vibrations are marked in bold, combination vibrations are not included in the table.

From a group theoretical approach, the S_1 -state should be of A_2' -symmetry. Therefore, only vibronic transitions which are induced by e' -modes are symmetry allowed.³⁶ As can be seen from Tab. 1, the experimental data are consistent with the calculated e' -modes within an error below 10 cm^{-1} for all three isotopomers.

In the first part (between 0 and 900 cm^{-1}) of the emission spectra, there are few, well separated vibronic bands, which undergo only minor changes upon deuteration. The atomic movement patterns, which can be evaluated from the DFT calculations, imply that these first six vibrations are deformation modes of the carbon skeleton. Another skeletal vibration is calculated to be located around 1020 cm^{-1} , but it is of low intensity and difficult to detect due to an intense combination vibration located at 1040 cm^{-1} . Although most of these modes involve the benzenoid as well as cyclobutadienoid rings, ν_1 in Tab. 1 at 100 cm^{-1} can be attributed directly to the latter. This scissoring-like vibration is characteristic for angular [N]phenylenes and has been found experimentally and theoretically for other [N]phenylenes,

too.³⁶ On closer inspection of the movement pattern, there is no change of bond angles or distances in the benzenoid rings. According to the calculations, this vibration is caused by a bond length change in the cyclobutadienoid rings (Fig. 3a), and can therefore be used as probe for the bond strength change between different states.

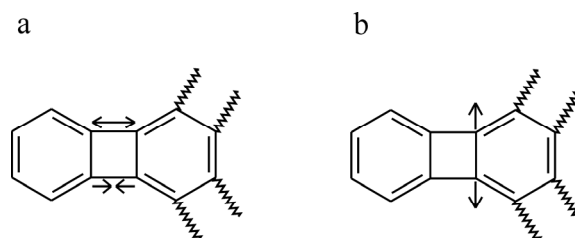


Fig. 3: Movement patterns of the probe vibrations ν_1 (a) and ν_{12} (b).

In the region of interest for CC stretch modes, e.g. 1000-1400 cm^{-1} , the spectra display a complex structure affected strongly by deuteration. CH vibrations, marked as bold lines in Fig. 2, can be identified readily due to their characteristic shifts upon deuteration. According to their frequency, the four CH modes ν_7 (991 cm^{-1}), ν_9 (1110 cm^{-1}), ν_{11} (1161 cm^{-1}) and ν_{13} (1279 cm^{-1}) in the emission spectrum of **(1)-h₁₂** should be CH bending modes. This assumption is confirmed by the DFT calculations. The corresponding vibrations for the deuterated isotopomers are given in Tab. 1. The shift factor of 1.3 fully agrees with the theoretical value of 1.36. The atomic movement pattern of ν_7 and ν_{13} affect only the α H-atoms and therefore the frequencies of the corresponding vibrations in **(1)-d₆** practically do not change (see Tab. 1).

Although ν_{15} and ν_{16} exhibit deuterium isotope shifts and are treated as CH vibrations in Fig. 2, they are not really CH modes. According to the DFT calculations, they constitute complex CC valence vibrations of the external phenyl rings and are affected by deuteration because the hydrogen atoms that are directly connected to the moving carbon atoms are also included in the vibration. Another benzenoid CC stretching mode (ν_{17}) is located at 1590 cm^{-1} .

Between 1000 and 1400 cm^{-1} , three fundamental CC valence vibrations (ν_{10} , ν_{12} and ν_{14}) are predicted by theory. These bands are found in the emission spectra around 1125, 1175 and 1360 cm^{-1} and are essentially not affected by deuteration. According to the DFT calculations, the last one of these is a complex vibration of the outer benzocyclobutadiene moieties and is of minor analytical value. The other two CC stretching modes can be assigned exclusively to the cyclobutadiene moieties. Unfortunately, ν_{10} is of very low intensity and, for **(1)-d₁₂**, can be barely discerned in the emission spectrum. The other band ν_{12} at 1175 cm^{-1} is assigned to a CC valence vibration associated mainly with the shared bond of fusion between the central

cyclohexatrienoid and cyclobutadienoid rings (Fig. 3b) and is therefore an excellent probe for the cyclobutadiene-cyclohexatriene interaction.

3.2 IR Spectra

For reliable assignment of the fundamental ground state vibrations, the results obtained by LESS and the DFT calculations are compared with the IR spectra of **(1)**-*h*₁₂, **(1)**-*d*₆ and **(1)**-*d*₁₂ (Fig. 4).

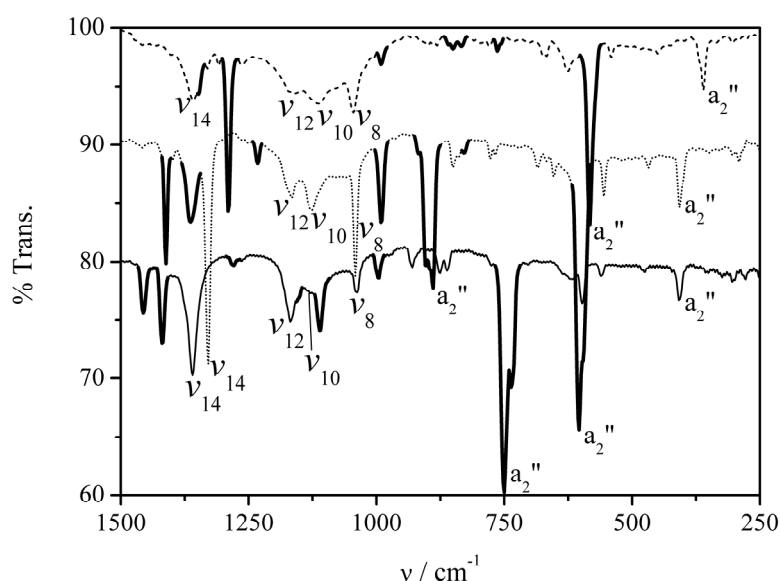


Fig. 4: IR-spectra of **(1)**-*h*₁₂ (solid), **(1)**-*d*₆ (dotted) and **(1)**-*d*₁₂ (dashed) in CsI. CC-vibrations between 1000 and 1500 cm⁻¹ and out-of-plane-modes are labeled, CH vibrations are marked as bold lines.

The frequencies are also given in Tab. 1. IR and LESS emission data are consistent within an error of about 5 cm⁻¹. In addition to e' vibrations, *a*₂'' modes are also IR active. The most prominent vibration of this class is the aromatic CH out-of-plane vibration located at 750 cm⁻¹ for **(1)**-*h*₁₂. In the IR spectrum of **(1)**-*d*₁₂, this band is shifted to 583 cm⁻¹. In **(1)**-*d*₆, the CH deformation band is split into two, one at 603 cm⁻¹, belonging to the CD vibration, and the other at 890 cm⁻¹, caused by the two isolated CH bonds.

3.3 Vibrational analysis of Shpol'skii excitation spectra

In the excitation spectra of **(1)**-*h*₁₂, **(1)**-*d*₆ and **(1)**-*d*₁₂, the same fundamental modes as in the emission spectra can be identified. These values are also given in Tab.1. A partial mirror image relationship exists for the emission and excitation spectra concerning the approximate

spectral positions of the vibronic bands. However, in comparison to the emission spectra, distinct modes in the excitation spectra are increasingly enhanced due to vibrational mixing with the S_2 -state, and combination vibrations are more pronounced than in the emission spectra, hampering the identification of fundamental modes at energies exceeding 1000 cm^{-1} . The excitation spectra between 1000 and 1400 cm^{-1} are shown in Fig. 5.

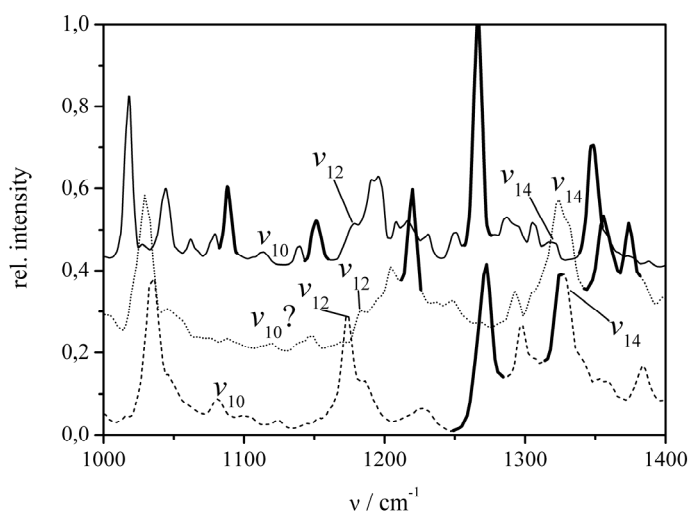


Fig. 5: Shpol'skii excitation spectra ($\lambda_{\text{em}} = 451\text{ nm}$) of **(1)- h_{12}** (solid), **(1)- d_6** (dotted) and **(1)- d_{12}** (dashed) at 4.2 K in octane. Vibrational energies (given in cm^{-1}) of the vibronic bands are referred to the 0-0 transition. CH vibrations are marked as bold lines. Intensities of the spectra are not corrected for excitation energy.

In Fig. 5, CH vibrational bands are again marked as bold lines. In the excitation spectra of **(1)- h_{12}** and **(1)- d_6** , the assignment of the probe vibration ν_{12} is not definite due to a combination band located at 1200 cm^{-1} , which is also present in the corresponding emission spectra at 1240 cm^{-1} , but absent in the spectra of **(1)- d_{12}** .

In the excitation spectra, fundamental modes $\nu_1 - \nu_{13}$ are all shifted $10\text{-}30\text{ cm}^{-1}$ to lower energies compared to the emission spectra. More pronounced differences are found for the CC stretching modes $\nu_{14} - \nu_{17}$. The only exception is the probe vibration ν_{12} , which remains constant.

3.4 Comparison of experimental and theoretical results

In addition to the experimental results, the S_1 -state structure of **(1)** was also computed. The calculated S_0 - and S_1 -state bond lengths and corresponding bond length changes are given in Fig. 6.

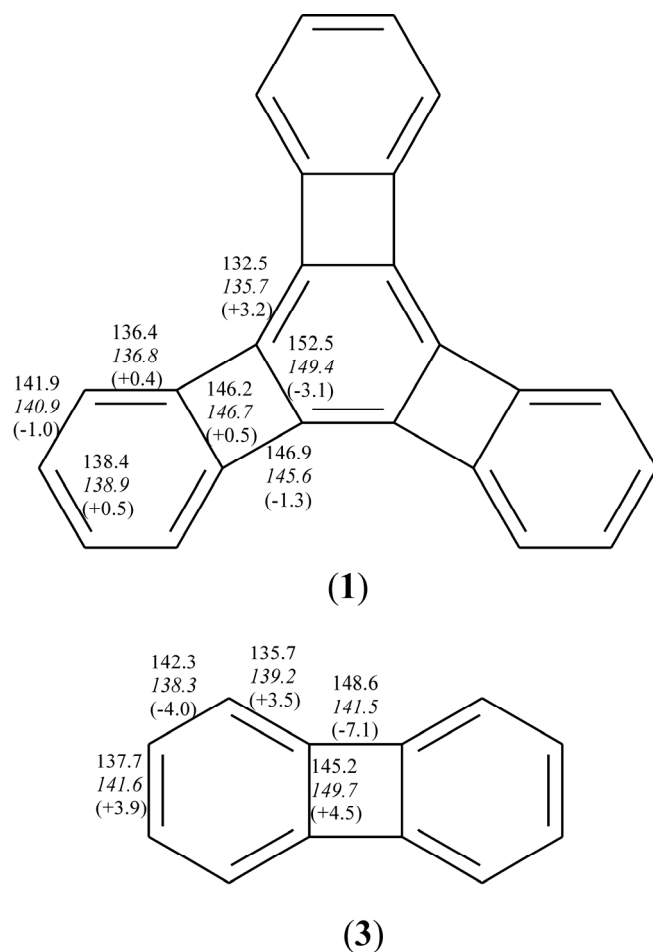


Fig. 6: Calculated bond lengths of the S_0 -state, the S_1 -state (in italic) and bond length differences (in brackets) of **(1)** and **(3)**, given in pm.

As depicted in Fig. 6, noticeable bond length changes are predicted only for the central six-membered ring, the changes in the periphery of the molecule being negligible. However, the average bond length change of 1.3 pm and the maximum bond length change of 3.2 pm are significantly less than the corresponding values for biphenylene **(3)**, 4.4 pm and 7.1 pm, respectively, also recorded in Fig. 6. In comparison to the ground state of **(1)**, in the S_1 -state the bonding π -orbitals are depopulated, whereas antibonding π^* -orbitals are populated, leading to an overall reduction of bond strength and bond order. Therefore, the energy of the vibronic bands in the excitation spectra is expected to be lower relative to those in the emission spectra. This effect can be observed for most bands present in the LESS excitation spectra of **(1)**, probe vibration ν_1 included.

Contrary to the expected reduction of π -bond strength, probe vibration ν_{12} displays an essentially different tendency compared to all other modes. This is connected to the special electronic configuration in the central ring. Like outlined in the introduction, in the ground state the bonds in the central ring are localized in a cyclohexatriene-type manner. The bonds

probed by ν_{12} represent quasi single bonds. This is supported by the energy of this vibration (1176 cm^{-1}), being located far below the corresponding values of aromatic CC stretch modes, which usually exceed 1400 cm^{-1} . As can be seen in Fig. 6, in the excited state these quasi single bonds are shortened, whereas the quasi double bonds are expanded. This reorganization of the central ring leads to a partial restoration of the benzene geometry as also predicted for the Siegel compound.⁵ If the π -system is distortive in the triangular [4]phenylene, too, an increase of σ -bond strength of the quasi single bonds is expected when the π -bond order is reduced by electronic excitation. This means that, for the probe vibration ν_{12} , the reduction of vibration energy (which is evident for the other modes due to reduction of π -bond order) is more or less cancelled by the increase of the σ -bond strength. This proposed symmetrization effect is in excellent agreement with the experimental data presented. In this context, it is interesting why (1) and (2) adopt a similar behaviour in the excited state, although the effect is remarkably smaller for (1). Unfortunately, the results provide no data for direct comparison with the Kekule mode discussed for aromatic systems like benzene or (2) because of different electronic structures of the S_1 -states. The DFT calculations show that for (1) no vibration corresponding to the (exalted) Kekule mode exists. This is not astonishing as the exalted Kekule mode strictly speaking requires two degenerated hypothetical D_{3h} structures, which for (1) surely are not given, since the central ring of (1) is not aromatic. Merely an a_1' vibration, which, according to the DFT-calculations, is located at 905 cm^{-1} , could be interpreted as "Kekule mode". This vibration is only raman active and is not accessible with LESS. However, from the DFT calculations it is expected, that this vibration does not induce any alterations in the length of the double bonds and therefore, can be considered as a CC stretch mode of the three isolated single bonds rather than an aromatic ring vibration.

3.5 Internal conversion rates of triangular [4]phenylenes

The extent of geometric distortion caused by electronic excitation is an important factor for the rate of internal conversion. The rate constants of internal conversion, k_{IC} , are determined mainly by the Franck-Condon factors $\langle \chi(S_0) | \chi(S_1) \rangle$, defined by the vibrational wave function $\chi(S_1)$ of the excited state and the wave function $\chi(S_0)$ of the vibrationally excited ground state. These Franck Condon factors are dominated by CH vibrations in the case of small geometry changes between S_0 - and S_1 -state.^{32,33} Therefore, for most polycyclic aromatic hydrocarbons (PAH), the important vibrations are the CH stretching modes. For PAH the CH induced internal conversion rate constants k_{IC} were in the order of 10^7 s^{-1} .^{32,33} For studying the influence of CH vibrations on the k_{IC} rates of [N]phenylenes, the fluorescence lifetimes of (1)-

h_{12} and $(\mathbf{1})\text{-}d_{12}$ have been measured at different temperatures in order to check the isotropic effect. It was expected to find smaller k_{IC} values for $(\mathbf{1})\text{-}d_{12}$, in case the internal conversion of $(\mathbf{1})$ is induced by CH vibrations.

The processes potentially relevant for the deactivation of $(\mathbf{1})$ are sketched in Fig. 7.

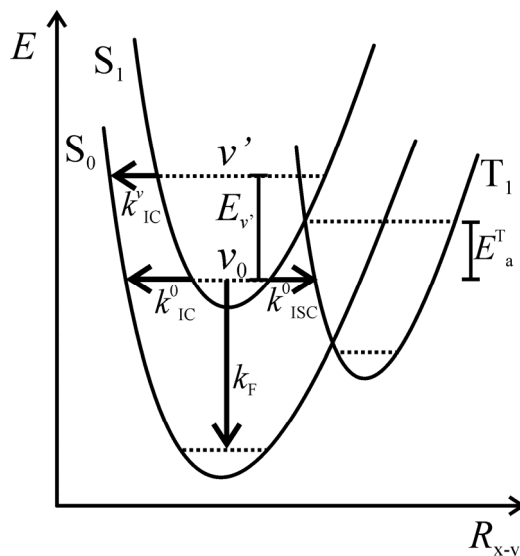


Fig. 7: Processes proposed for the S_1 -state deactivation of $(\mathbf{1})$.

The results shown in Fig. 8 were first evaluated using a monoexponential function according to a simple Arrhenius relationship. Only a poor agreement between experimental and fitted data was obtained. In a second approach the data were analysed using Eqn. 1, which yielded an excellent agreement. This further supports the model of two different temperature dependent processes, as depicted in Fig. 7.

If it is assumed that the fluorescence rate constant k_F and the vibrational ground state non-radiative rate constant, k_{NR}^0 (including internal conversion k_{IC}^0 and intersystem crossing k_{ISC}^0), are independent of temperature effects, the sum k_i over all deactivation processes can be expressed by Eqn. 1., if the internal conversion of vibrationally excited states is limited to only one vibronic state v' .

$$k_i = k_F + k_{NR}^0 + k_{IC}^v \cdot \exp(-E_{v'}/k_B T) + k_{ISC}^v \cdot \exp(-E_a^T/k_B T) \quad \text{Eqn. 1}$$

The value of k_F can be calculated from the room temperature fluorescence quantum yield and lifetime.³¹

The results, which were derived from a biexponential fit of the fluorescence lifetimes ($k_i = 1/\tau_F$) in dependence of temperature shown in Fig. 8, are given in Tab. 2.

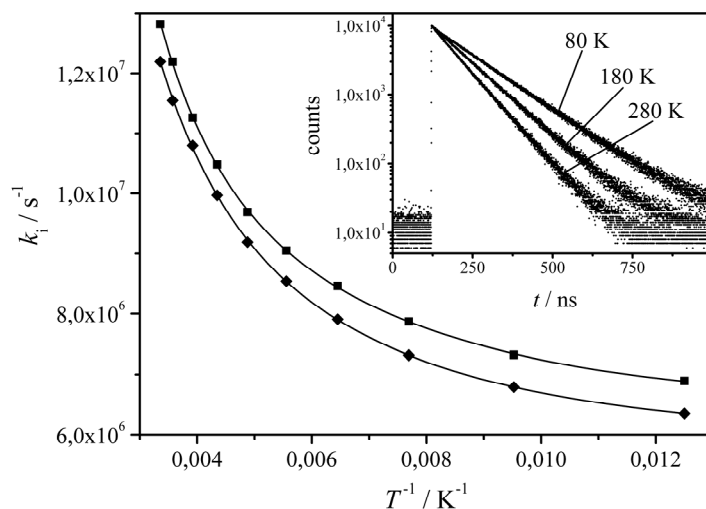


Fig. 8: Arrhenius plot of the deactivation rate constant k_i of **(1)**- h_{12} (!) and of **(1)**- d_{12} (Λ) in Me-THF in the temperature range 80 - 280 K ($\lambda_{\text{ex}} = 392$ nm, $\lambda_{\text{em}} = 475$ nm). The solid lines depict the biexponential fits derived from the model equation Eqn. 1. The experimental error is approximately ± 10 %. Inset: fluorescence decays of **(1)**- h_{12} .

	(1) - h_{12}	(1) - d_{12}
$k_i^{298\text{K}} / \text{s}^{-1}$	1.3×10^7	1.2×10^7
k_F / s^{-1}	1.9×10^6	1.9×10^6
$k_{\text{NR}}^0 / \text{s}^{-1}$	4.7×10^6	4.2×10^6
$k_{\text{IC}}^v / \text{s}^{-1}$	1.4×10^8	1.1×10^8
$k_{\text{ISC}}^v / \text{s}^{-1}$	1.3×10^7	1.5×10^7
$E_{v'} / \text{cm}^{-1}$	920	940

Tab. 2: Deactivation rate constants of **(1)**- h_{12} and **(1)**- d_{12} .

As can be seen from Tab. 2, k_{IC}^v is indeed smaller for **(1)**- d_{12} . Therefore, internal conversion of vibronically excited states ($S_1(v')$) of **(1)** is most probably induced by CH vibrations. Preliminary measurements of τ_F of 9,10-dimethyl-angular [3]phenylene at room temperature revealed that τ_F is not influenced by methylation of the middle ring as both, angular [3]phenylene and 9,10-dimethyl-angular [3]phenylene, exhibit τ_F of 20 ns.³¹ This indicates that the internal conversion of angular [N]phenylenes is induced by CH vibrations of the external, aromatic six membered rings. The small geometry deviation in **(1)** discussed in Section 3.4 is confirmed by the low k_{IC}^v ($6.4 \times 10^6 \text{ s}^{-1}$ at 298 K) and the discussed isotope effect

found in the temperature dependent lifetime measurements. In contrast, for biphenylene, a high k_{IC} of $4 \times 10^9 \text{ s}^{-1}$ and essentially no isotope effect on k_{IC} of biphenylene- d_8 was observed.^{34,35} This result, too, is consistent with the computational results presented in Fig. 6, giving evidence for a different internal conversion mechanism due to major geometry changes upon excitation.

The activation energy $E_{v'}$ is in the range of 900-950 cm^{-1} for both (1)- h_{12} and (1)- d_{12} no isotope effect on $E_{v'}$ is observable within the experimental accuracy. Therefore, v' is supposed to be a CC mode and for symmetry reasons, v' is expected to be a total symmetric (a_1') mode. Interestingly, on inspection of the reduced masses provided by the DFT calculations, there is only one a_1' -CC mode between 700 and 1300 cm^{-1} , namely the a_1' vibration located at 905 cm^{-1} in the ground state, which was assumed as closest to a Kekule mode-like vibration of (1). As already pointed out this a_1' vibration is not accessible with LESS and quantitative conclusions on this vibration in the excited state of (1) can not be drawn. However, from the temperature-dependent measurements it is attractive to assume, that this vibration is not exalted like the Kekule mode in benzene.

4. Summary

In this work the geometric effects in the molecule of triangular [4]phenylene (1) caused by electronic excitation were investigated. According to the PECI calculations there are only minor geometry changes between the S_0 - and the S_1 -state of (1). This is supported by the observed isotope effect on the internal conversion rates of (1), which suggests that internal conversion is likely to be induced by CH-vibrations, as expected for molecules with similar S_0 - and S_1 -structures. From the DFT calculations the most prominent geometry effects are expected for the cyclohexatrienoid central ring which should undergo a partial resymmetrization in the S_1 -state. This is confirmed by the analysis of the vibronic structure of the fluorescence emission and excitation spectra. However, the expected changes in bond lengths are relatively small (s. Figure 6). Although the results suggest similar geometry effects in the excited states of (1) and (2), more detailed theoretical data is necessary for proper interpretation of these results, which are in contrast to results reported for (3). Former studies with biphenylene revealed that, in contrast to the angular [N]phenylenes, the internal conversion of biphenylene is associated with major geometry changes between the S_0 - and S_1 -states, as also evident in the PECI calculations and the large Stokes shift in the absorption and fluorescence emission spectra. Future work will be concerned with the linear [N]phenylenes.

As preliminary studies indicate that these substances, such as biphenylene, undergo a completely different internal conversion mechanism. However, additional experimental data regarding the contribution of CC vibrations to the rate of internal conversion of linear [N]phenylenes are necessary for the verification of theoretical predictions.

Acknowledgement

This work was funded by the Fonds der Chemischen Industrie, NSF (CHE-0071887), the Deutscher Akademischer Austauschdienst (D/0103669), and the EU-Access to Research Infrastructures Programme (HPRI-CT-1999-00064). The Center for New Directions in Organic Synthesis is supported by Bristol-Myers Squibb as a Sponsoring Member and Novartis as a Supporting Member. The use of the computational facilities of the Regionale Rechenzentrum Erlangen (RRZE) is gratefully acknowledged. We thank Prof. Tim Clark, Erlangen, for discussions.

Preparative section

2,3,6,7,10,11-Hexadeutero-triangular [4]phenylene (**1**)-*d*₆.

Method A: To an NMR tube containing triangular [4]phenylene (4.0 mg, 0.013 mmol) in dry C₆D₆ (1.0 mL) under N₂ was added trifluoroacetic acid-*d* (0.3 mL). The resulting mixture was degassed by three successive freeze-pump-thaw cycles, the NMR tube sealed under vacuum and heated at 145 °C for 50 h. The dark reaction mixture was cooled, the solvent removed under reduced pressure and the black residue subjected to preparative thin layer chromatography, eluting with 15% dichloromethane/hexanes to give (**1**)-*d*₆ as yellow needles. (1.0 mg, 25%; mp = 247 °C).

Method B: To a solution of hexakis(trimethylsilyl)-(**1**) (96 mg, 0.13 mmol) in dry CDCl₃ (30 mL) was added trifluoroacetic acid-*d* (4.0 mL). The reaction mixture was stirred overnight at 25 °C under N₂ and subsequently washed with water (2 x 50 mL), brine (2 x 50 mL) and dried with MgSO₄. The solvent was removed under reduced pressure to give (**1**)-*d*₆ as a yellow powder. (36 mg, 90%; mp = 247 °C; IR (KBr) $\tilde{\nu}$ = 3061 (ν CH), 2265 (ν CD), 1412, 1328, 889 (δ CH), 603 (δ CD) cm⁻¹; MS (70 eV) *m/z* (rel. intensity) 306 (M⁺, 100); ¹H NMR (500 MHz, C₆D₆) δ 6.97 (s, 6H); ¹³C{¹H} NMR (100 MHz, CDCl₃) δ 148.5, 130.1, 128.2 (t, *J* = 24 Hz), 119.7.)

Hexakis(trimethylsilylethynyl)benzene, (4)

A solution of hexabromobenzene (1 g, 1.8 mmol), Pd(PPh₃)₂Cl₂ (110 mg, 0.16 mmol), CuI (30 mg, 0.16 mmol) and trimethylsilylethyne (2 ml, 20 mmol) in 15 ml triethylamine was heated in a glass bomb with Teflon stopcock in an oil bath at 120 °C. After 24 h, trimethylsilylethyne (1 ml, 10 mmol) was added, followed by another 1 ml of trimethylsilylethyne after an additional d. After 24 h, the solvent was removed under reduced pressure. Column chromatography on silica with hexane/CH₂Cl₂ (85:15) gave (3) as brown crystals. (230 mg, 20 %; ¹H- and ¹³C-NMR data were consistent with those reported in the literature.)⁵³

Triangular [4]phenylene-*d*₁₂, (1)-*d*₁₂

A suspension of KF (470 mg, 8 mmol) in 10 ml dimethoxyethane was stirred at room temperature for 5 min. D₂O (320 μl, 16 mmol) was added, and the suspension was again stirred for 5 min. Then, a solution of (4) (70 mg, 0.1 mmol) and 16-crown-8 (15 mg, 0.06 mmol) in 5 ml dimethoxyethane were added and the pale yellow solution removed from the solid KF·2D₂O after 15 min via syringe. This solution was mixed with CpCo(CO)₂ (20 μl, 0.15 mmol) and injected over 8 h to 10 ml of boiling bis(trimethylsilyl)ethyne. During the addition, the reaction mixture was irradiated with a slide projector lamp. Heating and irradiation were continued overnight. Dimethoxyethane was removed by rotary evaporation, and the bis(trimethylsilyl)ethyne was recovered by vacuum transfer. The residue was purified by column chromatography on silica with hexane/CH₂Cl₂ (85:15) to give hexakis(trimethylsilyl)-(1)-*d*₆ as a yellow oil.

The crude hexakis(trimethylsilyl)-(1)-*d*₆ was dissolved in a mixture of trifluoroacetic acid-*d* (1 ml, 170 mmol) and 6 ml chloroform and the solution was stirred for 24 h at room temperature. The volatiles were removed by vacuum transfer. Column chromatography of the residue on silica with hexane/CH₂Cl₂ (85:15) and recrystallization from hexanes gave (1)-*d*₁₂ as yellow needles. (6 mg, 18 %; D-incorporation ~ 98% by mass spectrometry; IR (CsI) $\tilde{\nu} = 2289$ (νCD), 1290, 582 cm⁻¹ (δCD); MS (70eV) *m/z* (rel. intensity) 312 (M⁺, 100).)

References

- 1 Y. Haas and S. Zilberg, *J. Am. Chem. Soc.*, 1995, **117**, 5387.
- 2 S. Shaik, P. C. Hiberty and G. Ohanessian, J.-M. Lefour, *J. Phys. Chem.*, 1988, **92**, 5086.
- 3 S. Shaik, A. Shurki, D. Danovich and P. C. Hiberty, *J. Am. Chem. Soc.*, 1996, **118**, 666.
- 4 S. Shaik, A. Shurki, D. Danovich and P. C. Hiberty, *Chem. Rev.*, 2001, **101**, 1501.
- 5 P. C. Hiberty and S. Shaik, *Phys. Chem. Chem. Phys.*, 2004, **6**, 224.
- 6 P. W. Fowler, R. W. A. Havenith, L. W. Jenneskens, A. Soncini and E. Steiner, *Chem. Commun.*, 2001, 2386.
- 7 Z. B. Maksić, D. Kovacek, M. Eckert-Maksić, M. Böckmann and M. Klessinger, *J. Phys. Chem.*, 1995, **99**, 6410.
- 8 P. von R. Schleyer, C. Maerker, A. Dransfeld, H. Jiao and N. J. R. van Eikema Hommes, *J. Am. Chem. Soc.*, 1996, **118**, 6317.
- 9 P. von R. Schleyer, H. Jiao, N. J. R. van Eikema Hommes, V. G. Malkin and O. L. Malkina, *J. Am. Chem. Soc.*, 1997, **119**, 12669.
- 10 P. von R. Schleyer, M. Manoharan, Z. X. Wang, B. Kiran, H. Jiao, R. Puchta and N. J. R. van Eikema Hommes, *Org. Lett.*, 2001, **3**, 2465.
- 11 J. M. Schulmann and R. L. Disch, *J. Am. Chem. Soc.*, 1996, **118**, 8470.
- 12 J. M. Schulman and R. L. Disch, *J. Phys. Chem. A*, 1997, **101**, 5596.
- 13 J. M. Schulmann, R. L. Disch, H. Jiao and P. von R Schleyer, *J. Phys. Chem. A*, 1998, **102**, 8051.
- 14 J. M. Schulman and R. L. Disch, *J. Phys. Chem. A*, 2003, **107**, 5223-5227.

- 15 E. Steiner and P. W. Fowler, *Int. J. Quant. Chem.*, 1996, **60**, 609.
- 16 B. C. Berris, G. H. Hovakeemian and K. P. C. Vollhardt, *J. Chem. Soc., Chem. Commun.* 1983, 502.
- 17 M. Hirthammer and K. P. C. Vollhardt, *J. Am. Chem. Soc.*, 1986, **108**, 2481.
- 18 L. Blanco, H. E. Helson, M. Hirthammer, H. Mestdagh, S. Spyroudis and K. P. C. Vollhardt, *Angew. Chem.*, 1987, **99**, 1276; *Angew. Chem. Int. Ed. Engl.*, 1987, **26**, 1246.
- 19 R. Diercks and K. P. C. Vollhardt, *Angew. Chem.*, 1986, **98**, 268., *Angew. Chem. Int. Ed. Engl.*, 1986, **25**, 266.
- 20 R. Diercks and K. P. C. Vollhardt, *J. Am. Chem. Soc.*, 1986, **108**, 3150.
- 21 R. H. Schmidt-Radde and K. P. C. Vollhardt, *J. Am. Chem. Soc.*, 1992, **114**, 9713.
- 22 R. Boese, A. J. Matzger, D. L. Mohler and K. P. C. Vollhardt, *Angew. Chem.*, 1995, **107**, 1630, *Angew. Chem., Int. Ed. Engl.* 1995, **34**, 1478.
- 23 C. Eickmeier, D. Holmes, H. Junga, A. J. Matzger, F. Scherhag, M. Shim and K. P. C. Vollhardt, *Angew. Chem.*, 1999, **111**, 856, *Angew. Chem. Int. Ed.*, 1999, **38**, 800.
- 24 A. Schleifenbaum, N. Feeder and K. P. C. Vollhardt, *Tetrahedron Lett.*, 2001, **42**, 7329.
- 25 D. T.-Y. Bong, L. Gentric, D. Holmes, A. J. Matzger, F. Scherhag and K. P. C. Vollhardt, *Chem. Commun.*, 2002, 278.
- 26 P. I. Dosa, G. D. Whitener, K. P. C. Vollhardt, A. D. Bond and S. J. Teat, *Org. Lett.*, 2002, **4**, 2075.

- 27 S. Han, D. R. Anderson, A. D. Bond, H. V. Chu, R. L. Disch, D. Holmes, J. M. Schulman, S. J. Teat, K. P. C. Vollhardt and G. D. Whitener, *Angew. Chem.*, 2002, **114**, 3361, *Angew. Chem. Int. Ed.*, 2002, **41**, 3227.
- 28 S. Han, A. D. Bond, R. L. Disch, D. Holmes, J. M. Schulman, S. J. Teat, K. P. C. Vollhardt and G. D. Whitener, *Angew. Chem.*, 2002, **114**, 3357, *Angew. Chem. Int. Ed.*, 2002, **41**, 3223.
- 29 D. L. Mohler, K. C. P. Vollhardt and S. Wolff, *Angew. Chem. Int. Ed.*, 1995, **34**, 563.
- 30 H.-D. Beckhaus, R. Faust, A. J. Matzger, D. L. Mohler, D. W. Rogers, C. Rüchardt, K. P. C. Vollhardt and S. Wolff, *J. Am. Chem. Soc.*, 2000, **122**, 7819.
- 31 C. Dosche, H.-G. Löhmansröben, A. Bieser, P. I. Dosa, S. Han, M. Iwamoto, A. Schleifenbaum and K. P. C. Vollhardt, *Phys. Chem. Chem. Phys.*, 2002, **4**, 2156.
- 32 J. B. Birks (ed.), *Organic Molecular Photophysics*, Vol. 1, Wiley, New York, 1975.
- 33 N. J. Turro, *Modern Molecular Photochemistry*, Benjamin/Cummings Publishing, 1978.
- 34 T. Elsaesser, F. Lärmer, W. Kaiser, B. Dick, M. Niemeyer and W. Lüttke, *Chem. Phys.*, 1988, **126**, 405.
- 35 M. Niemeyer, *Strahlungslose Desaktivierungsprozesse angeregter antiaromatischer Kohlenwasserstoffe*, Dissertation, Universität Göttingen, 1990.
- 36 C. Dosche, M. U. Kumke, F. Ariese, A. N. Bader, C. Gooijer, P. I. Dosa, S. Han, M. Miljanic, K. P. C. Vollhardt, R. Puchta, N. J. R. van Eikema Hommes, *Phys. Chem. Chem. Phys.*, 2003, **5**, 4563.
- 37 F. Vögtle, J. E. Schulz and K. Rissanen, *Chem. Commun.*, 1992, 120.
- 38 C. Pecile and B. Lunelli, *J. Chem. Phys.*, 1968, **48**, 1336.

- 39 I. Kautz, T. Koch, K. Malsch and G. Hohlneicher, *J. Mol. Struct.*, 1997, **417**, 223.
- 40 C.-L. Lin, S.-Y. Chu and M.-C. Ou, *J. Chin. Chem. Soc.*, 1998, **45**, 13.
- 41 L. A. Nakhimovsky, M. Lamotte and J. Jousset-Dubien, *Physical Science Data* 40, Elsevier, Amsterdam 1989.
- 42 F. Ariese, C. Gooijer and J. W. Hofstraat, Eds.: *Shpol'skii Spectroscopy and other Site-Selection Methods*, Wiley&Sons, New York, 2000.
- 43 Gaussian 98, Revision A. 11, M. J. Frisch, G. W. Trucks, H. B. Schlegel, G. E. Scuseria, M. A. Obb, J. R. Cheeseman, V. G. Zakrzewski, J. A. Montgomery, Jr., R. E. Stratmann, J. C. Burant, S. Dapprich, J. M. Millam, A. D. Daniels, K. N. Kudin, M. C. Strain, O. Farkas, J. Tomasi, V. Barone, M. Cossi, R. Cammi, B. Mennucci, C. Pomelli, C. Adamo, S. Clifford, J. Ochterski, G. A. Petersson, P. Y. Ayala, Q. Cui, K. Morokuma, D. K. Malick, A. D. Rabuck, K. Raghavachari, J. B. Foresman, J. Cioslowski, J. V. Ortiz, A. G. Baboul, B. B. Stefanov, G. Liu, A. Liashenko, P. Piskorz, I. Komaromi, R. Gomperts, R. L. Martin, D. J. Fox, T. Keith, M. A. Al-Laham, C. Y. Peng, A. Nanayakkara, M. Challacombe, P. M. W. Gill, B. Johnson, W. Chen, M. W. Wong, J. L. Andres, C. Gonzalez, M. Head-Gordon, E. S. Replogle and J. A. Pople, Gaussian Inc., Pittsburgh, PA, 2001.
- 44 W. Hehre, L. Radom, P. v. R. Schleyer and J. A. Pople: *Ab initio Molecular Orbital Theory*, Wiley, New York, 1986.
- 45 C. Lee, W. Yang and R. G. Parr, *Phys. Rev. B*, 1988, **37**, 785.
- 46 A. D. Becke, *J. Chem. Phys.*, 1993, **98**, 5648.
- 47 P. J. Stephens, F. J. Devlin, C. F. Chabalowski and M. J. Frisch, *J. Phys. Chem.*, 1994, **98**, 11623.
- 48 M. W. Wong, K. B. Wiberg and M. J. Frisch, *J. Chem. Phys.*, 1991, **95**, 8991.

- 49 J. J. Stewart, *J. Comput. Chem.*, 1989, **10**, 209.
- 50 VAMP 8.1 Build 32, T.Clark, A.Alex, B.Beck, F.Burkhardt, J.Chandrasekhar, P.Gedeck, A.H.C.Horn, M. Hutter, B. Martin, G. Rauhut, W. Sauer, T. Schindler, and T. Steinke, Erlangen 2002
- 51 T. Clark and J. Chandrasekhar, *Isr. J. Chem.*, 1993, **33**, 435.
- 52 T. Clark in Recent Experimental and Computational Advances in Molecular Spectroscopy, NATO-ASI Series C, Vol. 406, R. Fausto (ed.), Kluwer Academic Publishers, Dordrecht, (1993), p. 369.
- 53 R. Diercks, J. C. Armstrong, R. Boese and K. P. C. Vollhardt, *Angew. Chem. Int. Ed.*, 1986, **25**, 268.